Pakistan J. Zool., vol. 52(3), pp 885-892, 2020. **DOI**: https://dx.doi.org/10.17582/journal.pjz/20190912010908

Interaction of Strychni Semen Combined with Paeoniae Radix Alba after Transdermal Administration: Skin Permeation and Pharmacokinetics

Yun-Feng Liu, Yong-Mei Guan, Dan Chen, Jia-Le Chen, Chen Jin, Wei-Feng Zhu, Lu Wu and Li-Hua Chen*

Key Laboratory of Modern Preparation of Traditional Chinese Medicine of Ministry of Education. Jiangxi University of Traditional Chinese Medicine, Nanchang, China.

Article Information
Received 20 March 2019
Revised 22 May 2019
Accepted 01 October 2019
Available online 27 February 2020

Authors' Contribution
DC and JC performed experimental work. YL analysed the data and wrote the article. YG, LW and CJ managed and conducted the laboratory work. LC and WZ applied for grants and designed the experimental protocols.

Key words
Strychni semen, Paeoniae radix alba, Skin permeation, Pharmacokinetics

ABSTRACT

Studies on the interaction of the active constituents after Strychni Semen combined with Paeoniae Radix Alba. Following transdermal administration to mouse, the content alterations in paeoniflorin after application of a combination of Strychni Semen extract (SSE) and Paeoniae Radix Alba extract (PRAE) by *in vitro* skin permeation were observed. The penetration quantity, infiltration rate and skin retention quantity of paeoniflorin in co-administrated with SSE were increased significantly ($P<0.05$). In the skin and brain, the peak concentration (C_{max}) and the area under the concentration-time curve ($AUC_{0\to t}$) of brucine and strychnine in co-administrated with PRAE were decreased significantly ($P<0.05$), and the C_{max} and $AUC_{0\to t}$ of paeoniflorin in co-administrated with SSE increased significantly ($P<0.05$). These results showed that the co-administrated of SSE and PRAE can play an attenuation and synergistic effect.

INTRODUCTION

Strychni Semen (SS), the dried seeds of *Strychnos nux-vomica* L. belonging to the family Loganiaceae (Singh *et al*., 2012; Umar *et al*., 2015) are known for both their great clinical value and high toxicity in many Asian countries, which have been clinically used to relieve rheumatic pain, to reduce swelling, to improve blood circulation, and to ease allergic symptoms as well as other practical effects (Gu *et al*., 2014). However, many studies have reported potent neurotoxic effects on the central nervous system when humans are exposed to SS or its main ingredients (strychnine and brucine, Fig. 1). Because of their strong central excitatory effects and narrow therapeutic window, this has profoundly limited the full use of their therapeutic potential (Liu *et al*., 2015; García-Alcocer *et al*., 2005; McCool and Chappell, 2007).

Paeoniae Radix Alba (PRA), roots of *Paeonia lactiflora* Pall, belonging to the Paeoniaceae family (Cao *et al*., 2014), has been widely used as a traditional Chinese medicine (TCM) herb to relieve pain, unblock the meridian, activate blood (Wang *et al*., 2014; Yan *et al*., 2018). However, pharmacokinetics studies found that the main bioactive ingredients, paeoniflorin (Fig. 1), had a very low bioavailability (3–4%) (Tu *et al*., 2019). Some proprietary Chinese medicines that contain PRA are applied for external use in the clinic.

In clinical prescriptions, compatibility is a characteristic and advantage of TCM that plays a crucial role in ensuring the safe when use of toxic herbs. Through rational compatibility, TCM cannot only increase the therapeutic effect but can also eliminate or decrease drug toxicity in the clinic. The compatibility of SSE and RPAE means they are often clinically used to treat rheumatism, and clinical results have showed that PRAE can obviously reduce the toxicity of SSE, enhancing its central analgesic effect (Hou *et al*., 2017; Li *et al*., 2018).

It has been reported that the main bioactive components of SS, as liposoluble alkaloid, have the keen ability of percutaneous penetration and can also be used as natural traditional absorption enhancers (Chen *et al*., 2013). Along with promoting the penetration of paeoniflorin, SS plays an analgesic and anti-inflammatory effect and can provide a synergistic effect. It has also been shown that PRA is able to increase the activities of superoxide dismutase by decreasing the amount of nitric oxide and malondialdehyde through blocking anti-free radical damage and cytotoxicity and through improving the anti-inflammatory and immunomodulatory effects of SS, thereby reducing inflammation and pain (Jiang *et al*., 2011).

* Corresponding author: chlly98@163.com
0030-9923/2020/0003-0885 $ 9.00/0

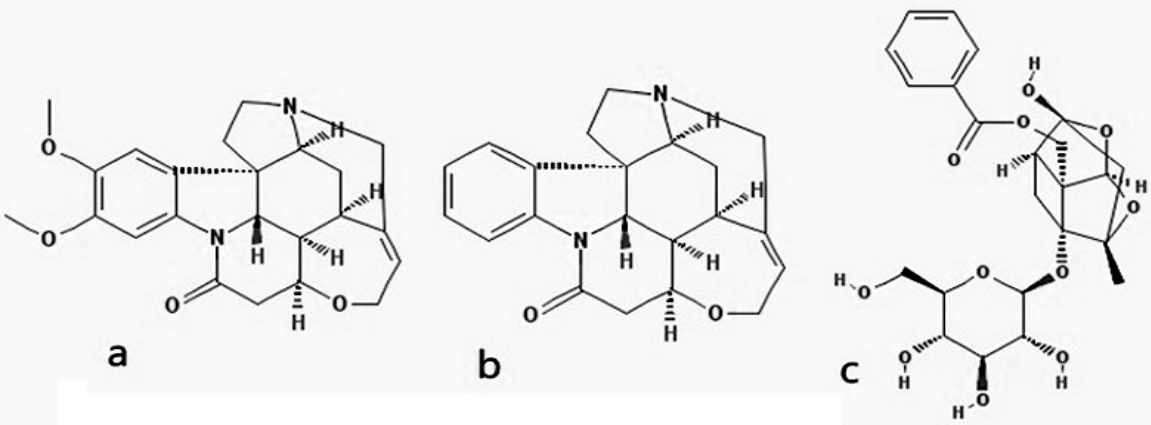

Fig. 1. Chemical structures of strychnine (a), brucine (b), and paeoniflorin (c).

There are a few studies on the protective effect of PRA on SS neurotoxicity, but they are mainly focused on detecting the potential toxicity constituent distribution in serum or tissue after oral administration (Shi *et al.*, 2017). These reports can partially verify or explain the rationality of their compatibility after oral administration. Transdermal administration is a common method of administration for the clinical use of SS. SS is typically used in modern medicines combined with PRA for the treatment of rheumatoid arthritis (Wang *et al.*, 2014), but there are no prior reports regarding skin permeation studies, microdialyses pharmacokinetics in transdermal drug delivery system.

In this manuscript, we explored the interaction behaviours of Strychni Semen extract (SSE) combine with Radix Paeoniae Alba extract (RPAE) for transdermal administration. We observed the content changes in paeoniflorin by permeation study through mice skin *in vitro* and compared the paeoniflorin, brucine and strychnine pharmacokinetic behaviours through the mice skin and brain by microdialyses after different RPAE-SSE compatibility assays *in vivo*.

MATERIALS AND METHODS

Materials

Strychni Semen, Paeoniae Radix Alba, were obtained from Nangchang Kaixinren Pharmacy Co., Ltd. (Strychni Semen, MQZ-2017-003, Paeoniae Radix Alba, BS-2017-002) (Nangchang, China). All herbs were identified by Professor Qianfeng Gong (Jiangxi University of Traditional Chinese Medicine). Phenacetin (≥98%, Shanghai Aladdin), tolbutamide (≥98%, Shanghai Aladdin), omeprazole (Dalian Mellon), chlorzoxazone (≥98%, Dalian Mellon), metoprolol (≥98%, Dalian Mellon), dapsone (≥98%, Shanghai Aladdin), carbamazepine (≥98%, The food and drug verification research institute of China), TRIS (Beijing Solarbio), NADPH (≥96%, Bejing Solarbio), glycerinum (≥98%, Shanghai Shenbo), PEG400 (Xilong Chemical Co.), methanol (TEDIA), acetonitrile (TEDIA), ultrapure water, BCA Kit (CWBIO) and poloxamer 407 (BASF, WPMI556B) were also obtained.

Kunming mice of clean grade (weighing 18-22 g, *In vitro* skin permeation study) were obtained from Hunan changsha SJA Laboratory Animal Co., Ltd. (Changsha, China), and raised under conditions with relative humidity (50% ± 3%) and ambient temperature (25±2°C), which were permitted free access to water and forage with a 12 h darkness/light cycles. All the animal experiments were carried out in accordance with the Institutional Guidelines for the Care and the Use of Laboratory Animals which approved by the Animal Ethics Committee of Jiangxi University of Traditional Chinese Medicine (approval ID: SYXK (Gan) 2007-0008).

Preparation of RPAE and SSE

The smashed and dried semen strychni was extracted three times with 6 volumes of 50% ethanol for 1 h each time under reflux, filtered and then concentrated by rotary evaporation. After that, the residue was dissolved in HCl (1 mol·L^{-1}) and centrifuged. The pH of supernatant was adjusted to 12. The solution was extracted with an equal volume of methylene chloride three times, and then these extractions were combined. Extracting solvent was centrifuged by rotary evaporator. Finally, the yield of SSE was determined by HPLC contain 17.70% brucine and 35.95% strychnine.

The Radix Paeoniae Alba was pulverized into coarse powder and was extracted two times with 7 volumes of ethanol, then added to reflux for 2 h each time, filtered,

concentrated and centrifuged. The supernatant was enriched by HPD100 macroporous resin with 30% ethanol. The eluate was concentrated under decompression and vacuum dried. RPAE yields as determined by HPLC contained 57.18% paeoniflorin.

Preparation of Azone/SSE/RPAE/SSE-RPAE gels

Based on our previous study, the SSE was dissolved in PEG400 (2 g), and then double distilled water was added slowly while stirring with a glass rod. In addition, poloxamer 407 (25%) was added into the SSE solution that was loaded at 1%, 3%, and 6%. Then, the mixture was stored overnight in the refrigerator (4°C). The second day, the mixture was placed at room temperature and the SSE gel was formed which contained 10mg/g SSE.

According to the same method, the Blank gel, Azone gel and three groups of RPAE gel. the RPAE groups contained 10mg/g, 30mg/g and 60mg/g RPAE, respectively.

The SSE-RPAE gels were prepared using the following method: the SSE was dissolved in PEG400 (2 g) and the RPAE was dissolved in water. The two solutions were then mixed at 1:1, 1:3 and 1:6 (SSE to RPAE) under continuous stirring. Then, poloxamer 407 (25%) was added into the mixed solution containing SSE (1%) and RPAE (1%, 3%, and 6%). The mixture was stored overnight at 4°C in the refrigerator. On the second day, the mixture was placed at room temperature, and three groups of SSE-RPAE gels (1:1, 1:3, 1:6) were formed, all of which contained 10mg/g SSE and 10mg/g, 30mg/g and 60mg/g PAER, respectively.

Skin permeation study of paeoniflorin in vitro

The mice (n=5) skins were obtained after the fur was removed with a shaver. After the subcutaneous fat was carefully removed from the abdominal skin, the skin was tailored to the same demensions and clamped between the donor and receptor cells. The medicated gel was painted on the stratum corneum evenly.

The *in vitro* permeation study of paeoniflorin across the mouse skin was assessed by using a vertical modified Franz diffusion cell system by means of a circulating water bath maintained at 37.0±0.5°C. The receiver chamber of the diffusion cell (orifice area of 1.85 cm^2, 12 mL) was filled with normal saline (recevier medium) and stirred at 150 rpm constantly. The solution (1 mL) was collected from the receptor cell and replaced with normal saline (1 mL) at designated time points (2, 4, 6, 8, 10, and 24 h) immediately (Zhao *et al*., 2018). Finally, the paeoniflorin were determined by HPLC analysis system within 24 h.

After the experiment, we removed and washed the drugs off the surface of the skin with normal saline. In addition, we cut off part of the skin on which the drugs were daubed, and it was then minced after After the addition of methanol (1 mL), the mixture was vortexed for 5 min and fragmented for 30 min by sonicator. Then, the supernatant was passed through a microporous membrane (0.22 μm) after centrifugation at 4000 r/min for 10 min in High Speed Refrigerated Centrifuge. Cumulative retention of the skin (Qs) was determined by HPLC analysis system.

Paeoniflorin was detected by using an Agilent HPLC system with an octadecylsilyl column (C18, 250 mm × 4.6 mm, 5 μm). The column temperature set at 30°C and the UV detector was set at 230 nm, the mobile phase was composed of phosphoric acid solution (volume ratio 0.1%) and acetonitrile (86:14, *v/v*) at a flow rate of 1.0 mL min^{-1}. Before automatic injection into the HPLC system, all the samples were passed through a microporous membrane (0.45 μm).

Local pharmacokinetic study in vivo

The mice (18-22 g, n=5) were implanted with a guide cannula using a s stereoscopic device under chloral hydrate anesthesia (10% induction). The fur was cleared away, and a midline incision was given to expose the skull subsequently. According to the following coordinates L / M = + 4.0 mm, A / P = +0.5 mm and D / V= − 3.5 mm (Sumbria *et al.*, 2011), a small hole was then drilled for the striatum from the bregma. The cannula was fastened to the skull with dental cement and two stainless steel screws. The mice were placed in individual test cages and allowed to adapt for 5–7 days before the experiment was statred (Uutela *et al*., 2009).

Mouse dorsal hair were removed with an electric shaver and depilatory cream was applied for 24 h before the experiment. The mice were briefly narcotized by chloral hydrate. Then, linear microdialysis probes were inserted under the skin with a microlance, and an active dialysis window was laid below the site of topical drug administration, and the linear probe was perfused continuously at a flow rate of 1.5 μL/min with Ringer's solution. The brain microdialysis probes were inserted into the striatum and were continuously perfused at a flow rate of 1.5 μL/min with sterile artificial cerebrospinal fluid (KCl 2.7mM, $CaCl_2$ 1.2mM, NaCl 145mM, $MgCl_2$ 1.0mM, pH 7.4) (Kao *et al*., 2015). The skin was permitted to balance for 30 min, and 1 g RPAE gel, SSE gel or SSE-RPAE gel was applied after the start of perfusion. The drug delivery area was 2 cm × 2.5 cm, with a dosing area surface covered with a polyethylene film block to prevent the gel from drying.

The dialysate samples were collected every 0.5 h in small vials and performed for 8 h, and then stored in low-temperature refrigerator at 80°C prior to detection of paeoniflorin, brucine and strychnine by LC-MS/MS

analysis system.

The dialysate samples *in vivo* were thawed at room temperature, and 30 μL aliquots of naringin solution (50 ng/mL in methanol) as an internal standard were added. After vortex mixing for 30 s, the aliquot (10 μL) was injected into the LC-MS/MS system directly. The HPLC analysis system consisted of a Shimadzu LC-30AD HPLC and vx C18 column (100 mm × 4.6 mm, 3.0 μM, Phenomenex Scientific Instrument Co. Ltd., Torrance, USA). For the dialysate samples *in vivo*, the flow rate was 0.5 mL/min, buffer A (10 mM ammonium acetate buffer) and buffer B (acetonitrile) were used for gradient elution as follows: 25% B (75% A) for 0.5 min, add to 65% B over 1.5 min, hold for 1 min, reduce to 25% B over 0.1 min, hold for 1.9 min (total time was 5 min). Column eluents were analyzed with an Applied Biosystems 4500 Triple Quad LC-MS/MS (Foster City, CA, USA) equipped with an electrospray probe interfaced to an LC and operating in electron spray, positive-multiple reaction monitoring (MRM) mode to monitor *m/z* 498.2→179 for paeoniflorin, *m/z* 335.2→184.2 for strychnine, *m/z* 395.3→324.4 for brucine and *m/z* 581.3→273.2 for naringin. There was no interference from endogenous material and the accuracy values and precision values were acceptable, the response of the detector was linear in the concentration range (1–600 ng/mL), and the mean correlation coefficient (*r*) for the calibration curve was over 0.99 for the plasma samples.

Statistical analysis

The pharmacokinetics parameters of paeoniflorin, strychnine and brucine concentration of plasma probe drugs versus time were analyzed by using DAS 2.0 Pharmacomechanical Intelligence Analysis Software (Drug and Statistics, prepared by the Chinese Pharmacological Society Mathematical Pharmacology Committee) and the statistical parameters were calculated. One-way ANOVA was performed using SPSS19.0 software for comparison of different pharmacokinetics data. For all analyses, P-values less than 0.05 are considered significantly different.

RESULTS

Permeation of paeoniflorin across mouse skin in vitro

The results showed that the cumulative permeation of paeoniflorin at 24 h increased after the compatibility of SSE and RPAE. The cumulative penetration rate in different compatibility proportions (1:1,1:3,1:6) of SSE-RPAE increased (by 2.38, 1.59, and 2.06 times). In addition, cumulative retention of the skin was also significantly increased after the compatibility of SSE and RPAE. The cumulative permeation and the cumulative penetration rate of the 1:6 compatibility gels were signally higher than those of the RPAE gel (P<0.05) (Fig. 2, Table I).

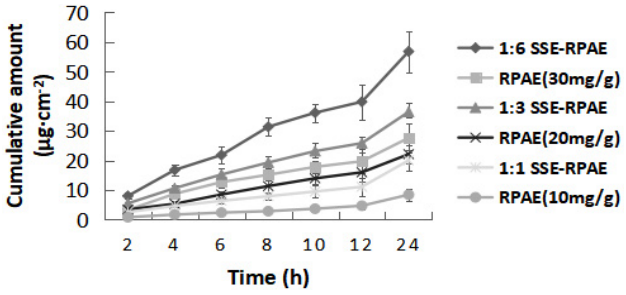

Fig. 2. *In vitro* mouse skin permeation profiles of paeoniflorin from different compatibility proportions.

Pharmacokinetic study in mice in vivo

This experiment inspected the microdialysis probe recovery rate by microdialysis sampling and the LC-MS/MS analysis coupling technique, generally comparing the skin and brain drug dynamic behavior after compatibility of SSE and RPAE.

In the skin, the C_{max} of brucine and strychnine in different proportions (1:1, 1:3, and 1:6) in the gels were decreased by 26.33%, 52.60%, 83.07% and 51.59%, 59.01%, 85.61%, respectively compared with the corresponding values in the control group. The $AUC_{0\rightarrow t}$ of brucine and strychnine was also decreased along with

Table I. *In vitro* mouse skin permeation parameters of paeoniflorin from different compatibility proportions.

Group		Q-t equation	r	Q_{24}(μg·cm^{-2})[a]	J_S(μg·cm^{-2}·h^{-1})[b]	Q_S(μg·cm^{-2})[c]
1:1	A	Q=0.3444t+0.2366	0.998	8.4028±0.5724	0.3444	0.8626±0.6539
	B	Q=0.7828t+0.2366	0.9989	20.0137±0.6532*	0.7828	1.6621±0.4249
1:3	A	Q=0.8556t+3.9244	0.9616	22.0958±0.3780	0.8556	1.7782±0.1924
	B	Q=1.3603t+6.5929	0.9635	36.4041±0.2742	1.3603	2.6033±0.1832*
1:6	A	Q=1.0278t+5.2898	0.9499	27.5973±0.2022	1.0278	2.0778±0.2298
	B	Q=2.1444t+9.8776	0.9608	56.8349±0.4042*	2.1444	3.0670±0.1917*

a, Cumulative amount permeated at 24 h; b, Cumulative penetration rate within 24 h; c, Cumulative retention of skin after 24h; *Significantly different from the 'A' group (P < 0.05); A, RPAE gel, B, SSE-RPAE gel.

the increase in the compatibility proportion. In the brain, the C_{max} of brucine in different proportions in the gels were decreased by 21.74%, 22.37% and 33.11% times, respectively. The C_{max} of strychnine in different proportions (1:3, 1:6) of SSE-RPAE was decreased significantly, and the $AUC_{0\rightarrow t}$ of strychnine in the 1:6 compatibility gel was significantly decreased by 33.45%, as shown in Fig. 3 (A, B, C, D) and Table II.

In the skin, the C_{max} and $AUC_{0\rightarrow t}$ of paeoniflorin in different proportions (1:1, 1:3, 1:6) of SSE-RPAE were increased by 3.79, 1.17, 2.01 times and 1.74, 1.34, 1.74 times, respectively. In the brain, the C_{max} and $AUC_{0\rightarrow t}$ of paeoniflorin in different proportions (1:1, 1:3, 1:6) gels were increased by 3.11, 1.92, 3.37 times and 3.39, 2.23, 3.02 times, respectively as shown in Figsures 3E and F and Table II.

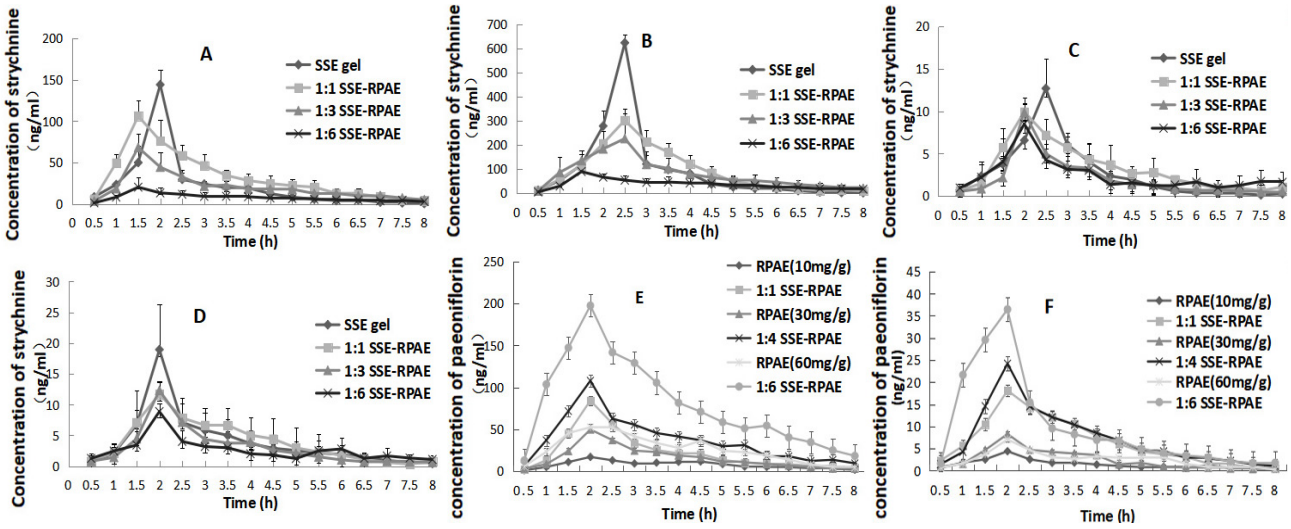

Fig. 3. Mean concentration-time profiles of the *in vivo* pharmacokinetic study after transdermal administration of different proportions of gels; (A): brucine in skin; (B): strychnine in skin; (C): brucine in brain; (D): strychnine in brain; (E): paeoniflorin in the skin; (F): paeoniflorin in the brain.

DISCUSSION

The compatibility of SS and PRA during transdermal delivery could help brucine and strychnine to exert local effect while reducing the concentration of the drugs entering the circulatory system, thereby reducing their toxicity (Li *et al*., 2018). Brucine and strychnine belong to the group of monoterpenoid alkaloids, which are alkaline. Paeoniflorin belongs to the group of bicyclic monoterpenoids, and p-gp-mediated efflux, and hydrolysis via a glucosidase might be the reason of paeoniflorin poor bioavailability (Liu *et al*., 2006).

In our previous study, in which we studied *in vitro* transdermal absorption of two alkaloids (brucine and strychnine) after the combination of SSE and RPAE, we found that RPAE could reduce the brucine and strychnine through compatibility, and the best ratio was 1:6 (Chen *et al*., 2016). In the *in vitro* skin permeation study, RPAE provided a low cumulative permeation of paeoniflorin at 24 h and low skin flux of paeoniflorin. With the combined use of SSE and RPAE, the penetration quantities, infiltration rate and skin retention rate of paeoniflorin were all significantly in different proportions of gels increased. In our earlier experiment, it was found that the results of transdermal permeation *in vitro*, the cumulation penetration of paeoniflorin increased after compatibility, which is consistent with the findings of a previous study that Azone can make skin keratinocytes swell (Fox *et al*., 2011). It was speculated that when SSE is combined with RPAE, the cells of the stratum corneum were changed from a fine arrangement to a loose arrangement, and the distance between the cells enlarged, which caused shedding of the outer layer of the stratum corneum, reduced the shielding effect of the skin against the drug and increased the penetration of paeoniflorin (Chantasart and Li, 2012). In addition, as the free volume of keratinocytes was increased, the degree of hydration of keratinocytes and the storage space of the drug were increased, which also explained why the retention of paeoniflorin in the skin was also increased after compatibility.

The pharmacokinetics behavior of RPAE, SSE, SSE-RPAE after topical application was studied by using microdialysis probes in the skin and brain *in vivo*, which were implanted precisely in the dermis to measure drug

Table II. Pharmacokinetic parameters of paeoniflorin, brucine and strychnine concentration-time courses in the skin and brain.

Constituent	Position	Parameters	A (RPAE=10mg/g)	B (1:1 SSE-RPAE)	A (RPAE=30mg/g)	B (1:3 SSE-RPAE)	A (RPAE=60mg/g)	B (1:6 SSE-RPAE)
paeoniflorin	Skin	C_{max}(ng/mL)	17.576±3.917	84.246±15.243**	49.74±11.396	107.944±24.726**	65.526±20.913	197.56±56.001**
		T_{max}(h)	1.9±0.224	2.1±0.224	2.1±0.224	2.1±0.224	2±0.354	2.1±0.224
		$T_{1/2}$(h)	0.891±0.388	1.331±0.837	1.1552±0.606	1.4958±0.608	0.801±0.461	1.252±0.348
		$AUC_{0\text{-}8h}$ ($ng\cdot h\cdot mL^{-1}$)	57.828±9.607	158.505±26.77**	132.457±40.524	309.964±44.228**	214.677±71.52	588.254±126.077**
		$AUC_{0\text{-}\infty}$ ($ng\cdot h\cdot mL^{-1}$)	61.698±11.699	161.385±30.387	148.721±40.524	353.422±67.985	221.618±67.927	624.334±144.792
		$MRT_{0\text{-}8h}$(h)	3.742±0.189	3.129±0.102	3.149±0.305	3.262±0.219	3.352±0.331	3.503±0.341
		$MRT_{0\text{-}\infty}$(h)	3.192±0.085	4.164±0.462	3.2572±0.744	4.566±1.785	3.579±0.684	3.85±0.3
	Brain	C_{max}(ng/mL)	4.374±2.861	17.978±6.709*	8.28±2.673	24.194±2.648**	8.34±0.708	36.44±3.066**
		T_{max}(h)	2±0	2.1±0.224	1.9±0.224	2.1±0.224	2.1±0.224	1.9±0.224
		$T_{1/2}$(h)	1.109±0.862	0.843±0.23	1.331±0.206	1.026±0.405	1.57±1.188	1.117±0.563
		$AUC_{0\text{-}8h}$ ($ng\cdot h\cdot mL^{-1}$)	10.72±7.565	47.024±9.063**	19.286±6.79	62.278±6.329**	20.429±6.525	82.15±11.097**
		$AUC_{0\text{-}\infty}$ ($ng\cdot h\cdot mL^{-1}$)	11.674±7.615	47.822±8.915	20.228±5.966	65.426±6.202	21.897±6.771	84.969±10.321
		$MRT_{0\text{-}8h}$(h)	3.529±0.417	3.27±0.228	3.325±0.388	3.034±0.186	3.374±0.394	2.665±0.172
		$MRT_{0\text{-}\infty}$(h)	4±0.402	3.372±0.293	3.704±0.863	3.431±0.246	3.772±0.61	2.925±0.271
			SSE	(1:1 SSE-RPAE)		(1:3 SSE-RPAE)		(1:6 SSE-RPAE)
Brucine	Skin	C_{max}(ng/mL)	143.978±18.177	106.074±19.399*		68.25±16.547*		24.376±8.733*
		T_{max}(h)	1.9±0.224	1.6±0.224		1.7±0.274		1.6±0.224
		$T_{1/2}$(h)	0.744±0.592	0.77±0.231		1.415±0.284		1.569±0.983
		$AUC_{0\text{-}8h}$ ($ng\cdot h\cdot mL^{-1}$)	188.335±54.201	170.208±77.261		180.746±35.013		68.151±27.548*
		$AUC_{0\text{-}\infty}$ ($ng\cdot h\cdot mL^{-1}$)	189.338±55.147	173.981±79.36		192.558±34.581		78.773±42.814
		$MRT_{0\text{-}8h}$(h)	2.558±0.285	2.917±0.203		3.095±0.236		3.137±0.496
		$MRT_{0\text{-}\infty}$(h)	2.577±0.283	3.046±0.17		3.113±0.297		3.026±0.326
	Brain	C_{max}(ng/mL)	12.676±3.517	9.92±1.649		9.84±1.032		8.48±2.416
		T_{max}(h)	2.3±0.274	2.1±0.224		2.1±0.224		2.1±0.224
		$T_{1/2}$(h)	0.678±0.274	0.795±0.385		1.428±0.462		1.815±1.736
		$AUC_{0\text{-}8h}$ ($ng\cdot h\cdot mL^{-1}$)	19.444±2.323	24.311±5.376		16.234±2.307		19.464±7.022
		$AUC_{0\text{-}\infty}$ ($ng\cdot h\cdot mL^{-1}$)	19.61±2.507	25.347±5.331		17.266±2.755		24.909±10.432
		$MRT_{0\text{-}8h}$(h)	2.955±0.197	3.298±0.171		3.13±0.1		3.364±0.34
		$MRT_{0\text{-}\infty}$(h)	3.06±0.286	3.671±0.373		3.632±0.238		4.534±1.429
Strychnine	Skin	C_{max}(ng/mL)	622.317±33.579	301.238±46.37*		255.118±45.912*		89.552±27.073*
		T_{max}(h)	2.4±0.224	2.6±0.224		2.3±0.447		1.5±0.235
		$T_{1/2}$(h)	0.577±0.234	1.949±1.148		2.084±1.44		3.101±1.25
		$AUC_{0\text{-}8h}$ ($ng\cdot h\cdot mL^{-1}$)	697.696±60.892	665.51±122.906		586.364±157.859		319.742±85.782*
		$AUC_{0\text{-}\infty}$ ($ng\cdot h\cdot mL^{-1}$)	698.905±61.509	695.335±116.009		632.56±152.178		406.315±152.384
		$MRT_{0\text{-}8h}$(h)	2.764±0.048	3.245±0.062		3.36±0.289		3.466±0.056
		$MRT_{0\text{-}\infty}$(h)	2.778±0.044	3.67±0.063		4.003±0.248		5.227±1.21
	Brain	C_{max}(ng/mL)	18.936±7.32	12.308±1.348		11.498±1.916*		8.854±1.301*
		T_{max}(h)	2.1±0.224	2.1±0.224		2.1±0.224		2.1±0.224
		$T_{1/2}$(h)	0.839±0.218	0.954±0.511		1.881±1.568		1.721±1.519
		$AUC_{0\text{-}8h}$ ($ng\cdot h\cdot mL^{-1}$)	30.681±9.467	32.634±12.273		23.346±2.705		20.419±4.56*
		$AUC_{0\text{-}\infty}$ ($ng\cdot h\cdot mL^{-1}$)	31.195±9.43	33.164±12.141		24.978±3.355		22.98±5.915
		$MRT_{0\text{-}8h}$(h)	3.078±0.365	2.991±0.312		3.112±0.311		3.491±0.52
		$MRT_{0\text{-}\infty}$(h)	3.203±0.438	3.182±0.265		3.728±0.737		4.47±1.218

Note: *Significantly different from the 'A' group ($P < 0.05$); **Significantly different from the 'A' group ($P < 0.01$); A: RPAE gel, B: SSE-RPAE gel.

molecules exacted in the extracellular fluid of the dermal layer where the paeoniflorin accumulated (Zhang *et al*., 2014). Analysis with an *in vivo* microdialysis sample from the skin and brain revealed that the C_{max} and $AUC_{0\rightarrow t}$ of brucine and strychnine in different SSE-RPAE proportions gels were decreased significantly, while the C_{max} and $AUC_{0\rightarrow t}$ of paeoniflorin were increased significantly. In conclusion, we can infer that the compatibility of SS and PRA promotes the penetration of paeoniflorin and limits the absorption of brucine and strychnine, which is consistent with the results of transdermal permeation *in vitro*.

CONCLUSIONS

SSE-RPAE promoted the cumulative permeation, penetration rate and skin retention rate of paeoniflorin *in vitro* permeation studies. Combined with our previous study, we found that the penetration quantities, infiltration rate and skin retention rate of brucine and strychnine in different proportions (1:1, 1:3, 1:6) of SSE-RPAE were all decreased significantly ($P<0.05$) after combination (Chen *et al*., 2016). These results were further verified in the skin and brain pharmacokinetics studies. The study results cannot only improve the clinical therapeutic use of SS but can also facilitate the exploration of possible preventative methods to decrease the toxic effects of SS through its combination with PRA. This is a better approach to the clinical application of SS and can expand the application of PRA, which is commonly used in the clinic as a reducing agent, combined with other noxious Chinese herbal medicines.

ACKNOWLEDGMENT

This research was funded by the National Natural Science Foundation of China (Grant no. 81760717, 81460606).

Statement of conflicts of interest

The research was undertaken in the absence of any commercial or financial relationships that could be construed as a potential conflict of interest.

REFERENCES

Cao, G., Li, Q., Cai, H., Tu, S. and Cai, B., 2014. Investigation of the chemical changes from crude and processed paeoniae radix alba-atractylodis macrocephalae rhizoma herbal pair extracts by using Q exactive high-performance benchtop quadrupole-orbitrap LC-MS/MS. *Evid. based Compl. Alt.,* **2014:** 1-14. https://doi.org/10.1155/2014/170959

Chantasart, D. and Li, S.K., 2012. Structure enhancement relationship of chemical penetration enhancers in drug transport across the Stratum Corneum. *Pharmaceutics,* **4:** 71-92. https://doi.org/10.3390/pharmaceutics4010071

Chen, J., Hu, W., Qu, Y., Dong, J., Gu, W., Gao, Y., Fang, Y., Fang, F., Chen, Z. and Cai, B., 2013. Evaluation of the Pharmacodynamics and Pharmacokinetics of Brucine Following Transdermal Administration. *Fitoterapia,* **86:** 193-201. https://doi.org/10.1016/j.fitote.2013.03.007

Chen, L.H., Chen, J.L., Wen, S.J., Guan, Y.M., Liu, L.L., Zhu, W.F. and Yang, M., 2016. Preparation of total alkaloids of strychni semen-total qlucosides of paeony gel and its transdermal absorption. *Chinese Pharmaceut. J.,* **51**: 1953-1957.

Fox, L., Gerber, M., Du Plessis, J. and Hamman, J., 2011. Transdermal drug delivery enhancement by compounds of natural origin. *Molecules,* **16:** 10507-10540. https://doi.org/10.3390/molecules161210507

García-Alcocer, G.Martínez-Torres, A. and Miledi, R., 2005. Strychnine induces embryotoxicity in rat neurulation. *Neurotoxicol. Teratol.,* **27:** 855-859. https://doi.org/10.1016/j.ntt.2005.06.020

Gu, L., Wang, X., Zhang, Y., Jiang, Y., Lu, H., Bi, K. and Chen, X., 2014. Determination of 12 potential nephrotoxicity biomarkers in rat serum and urine by liquid chromatography with mass spectrometry and its application to renal failure induced by semen strychni. *J. Sep. Sci.,* **37:** 1058-1066. https://doi.org/10.1002/jssc.201400053

Hou, C., Zhang, R., Zhang, K. and Chen, X., 2017. Total glycosides of paeony shows neuroprotective effects against semen strychni-induced neurotoxicity by recovering secretion of hormones and improving brain energy metabolism. *Metab. Brain Dis.,* **32:** 2033-2044. https://doi.org/10.1007/s11011-017-0082-5

Jiang, D., Chen, Y., Hou, X., Xu, J., Mu, X. and Chen, W. 2011. Influence of *Paeonia lactiflora* roots extract on cAMP-phosphodiesterase activity and related anti-inflammatory action. *J. Ethnopharmacol.,* **137:** 914-920. https://doi.org/10.1016/j.jep.2011.07.020

Kao, C.Y., Stalla, G., Stalla, J., Wotjak, C.T. and Anderzhanova, E. 2015. Norepinephrine and corticosterone in the medial prefrontal cortex and hippocampus predict PTSD-like symptoms in mice. *Eur. J. Neurosci.,* **41:** 1139-1148. https://doi.org/10.1111/ejn.12860

Li, S., Chu, Y., Zhang, R., Sun, L. and Chen, X. 2018.

Prophylactic neuroprotection of total glucosides of paeoniae radix alba against semen strychni-induced neurotoxicity in rats: Suppressing oxidative stress and reducing the absorption of toxic components. *Nutrients,* **10:** 514. https://doi.org/10.3390/nu10040514

Liu, F., Wang, X., Han, X., Tan, X. and Kang, W., 2015. Cytotoxicity and DNA interaction of brucine and strychnine—Two alkaloids of Semen Strychni. *Int. J. Biol. Macromol.,* **77:** 92-98. https://doi.org/10.1016/j.ijbiomac.2015.03.017

Liu, Z. Q., Jiang, Z. H., Liu, L. and Hu, M., 2006. Mechanisms responsible for poor oral bioavailability of paeoniflorin: Role of intestinal disposition and interactions with sinomenine. *Pharm. Res.,* **23:** 2768-2780. https://doi.org/10.1007/s11095-006-9100-8

McCool, B.A. and Chappell, A., 2007. Strychnine and taurine modulation of amygdala-associated anxiety-like behavior is 'State' dependent. *Behav. Brain Res.,* **178:** 70-81. https://doi.org/10.1016/j.bbr.2006.12.002

Shi, H., Hou, C., Gu, L., Xing, H., Zhang, M., Zhao, L., Bi, K. and Chen, X., 2017. Investigation of the protective effect of *Paeonia lactiflora* on semen strychni-induced neurotoxicity based on monitoring nine potential neurotoxicity biomarkers in rat serum and brain tissue. *Metab. Brain Dis.,* **32,** 133-145. https://doi.org/10.1007/s11011-016-9894-y

Singh, A., Saharan, V., Ram, V., Bhandari, A. and Bhati, R., 2012. Strychnos Nux-Vomica seeds: Pharmacognostical standardization, extraction, and antidiabetic activity. *J. Ayurveda Integr. Med.,* **3:** 80. https://doi.org/10.4103/0975-9476.96523

Sumbria, R., Klein, K.J. and Bickel, U., 2011. Acute depression of energy metabolism after microdialysis probe implantation is distinct from ischemia-induced changes in mouse brain. *Neurochem. Res.,* **36:** 109-116. . https://doi.org/10.1007/s11064-010-0276-2

Tu, J., Guo, Y., Hong, W., Fang, Y., Han, D., Zhang, P., Wang, X., Körner, H. and Wei, W., 2019. The regulatory effects of paeoniflorin and its derivative paeoniflorin-6′-o-benzene sulfonate CP-25 on inflammation and immune diseases. *Front. Pharmacol.,* **10**: 57. https://doi.org/10.3389/fphar.2019.00057

Umar, D., Veena, V., Hashim, A., Bahija, B., Kusai, B. and Mohammed, R., 2015. A reverse phased high-pressure liquid chromatographic method for the estimation of a poisonous matter in strychnos nux-vomica. *J. Adv. Pharmaceut. Technol. Res.,* **6:** 108. https://doi.org/10.4103/2231-4040.161506

Uutela, P., Karhu, L., Piepponen, P., Käenmäki, M., Ketola, R.A. and Kostiainen, R., 2009. Discovery of dopamine glucuronide in rat and mouse brain microdialysis samples using liquid chromatography tandem mass spectrometry. *Anal. Chem.,* **81:** 427-434. https://doi.org/10.1021/ac801846w

Wang, X., Wei, S., Liu, T., Pang, J., Gao, N., Ding, D., Duan, T., Cao, Y., Zheng, Y. and Zhan, H., 2014. Effectiveness, medication patterns, and adverse events of traditional chinese herbal patches for osteoarthritis: A systematic review. *Evid. based Compl. Alt.,* **2014:** 343176. https://doi.org/10.1155/2014/343176

Yan, B., Shen, M., Fang, J., Wei, D. and Qin, L., 2018. Advancement in the chemical analysis of *Paeoniae radix* (Shaoyao). *J. Pharmaceut. Biomed.,* **160:** 276-288. https://doi.org/10.1016/j.jpba.2018.08.009

Zhang, Y., Feng, N., Shen, L. and Zhao, J. 2014. Evaluation of psoralen ethosomes for topical delivery in rats by using *in vivo* microdialysis. *Int. J. Nanomed.,* **1:** 669. https://doi.org/10.2147/IJN.S57314

Zhao, Y., Fan, H.H., Zhu, J.H., Li, Y.H., Yang, X.Y., Deng, L.J., Li, W.D., Yang, M. and Li, R.B., 2019. Pharmacokinetic and tissue distribution of the innovative calcium sensitizer-M6 using an high performance liquid chromatography-ultraviolet test method in rats, Nanosci. *Nanotech. Lett.,* **11**: 258-264. http://doi.org/10.1166/nnl.2019.2875